Available online at www.eccomasproceedia.org
Eccomas Proceedia COMPDYN (2023) 3916-3925

ECCOMAS
Proceedia

COMPDYN 2023
9th ECCOMAS Thematic Conference on
Computational Methods in Structural Dynamics and Earthquake Engineering
M. Papadrakakis, M. Fragiadakis (eds.)
Athens, Greece, 12-14 June 2023

PERFORMANCE COMPARISON OF MASONRY WALLS WITH RECTANGULAR BRICKS AND INTERLOCKING BRICKS − STATIC LOADING TEST AND DYNAMIC ANALYSIS USING DEM –

A. Furukawa[1] and J. Kiyono[2]

[1] Department of Urban Management, Kyoto University
Kyotodaigaku-katsura, Nishikyo-ku, Kyoto 615-8540, JAPAN
e-mail: furukawa.aiko.3w@kyoto-u.ac.jp

[2] Department of Urban Management, Kyoto University
Kyotodaigaku-katsura, Nishikyo-ku, Kyoto 615-8540, JAPAN
e-mail: kiyono.junji.5x@kyoto-u.jp

Abstract

Masonry structures are commonly used in developing countries due to their inexpensiveness and material availability. Masonry structures are strong in resisting gravitational force but vulnerable to lateral forces such as earthquakes. Therefore, reinforcement for masonry structures in earthquake-prone areas is necessary. This paper considers using interlocking bricks instead of regular rectangular bricks as a reinforcement measure for masonry structures as it does not require extra material and is easy to implement. The effectiveness of interlocking bricks instead of regular rectangular bricks is examined by comparing the performance against static loading test and dynamic analysis results using DEM. The static loading test compares the load-displacement relationship of the masonry wall with rectangular bricks and the wall with interlocking bricks. The dynamic analysis results compare the collapse behavior against sinusoidal input between the masonry wall with rectangular bricks and the wall with interlocking bricks in both in-plane and out-of-plane directions. The performance of rectangular bricks and interlocking bricks are compared, and the effectiveness of using interlocking bricks instead of rectangular bricks is discussed.

Keywords: Masonry wall, Rectangular brick, Interlocking brick, Static loading test, Distinct element method.

ISSN:2623-3347
Peer-review under responsibility of the organizing committee of COMPDYN 2023.
doi: 10.7712/120123.10690.20105

1 INTRODUCTION

It is reported that 75% of the deaths caused by earthquakes are due to collapsed buildings and that most of the deaths caused by collapsed buildings are due to collapsed masonry structures with low earthquake resistance, often constructed in developing regions [1]. Although masonry structures are extremely vulnerable to seismic shaking, they are still being built worldwide today, especially in developing regions [2][3], because of their inexpensive materials, easy construction, and excellent heat and moisture insulation properties. There is a need for inexpensive and easy-to-construct seismic retrofitting methods for masonry structures.

Some of the existing studies on seismic strengthening methods for masonry structures have proposed the use of steel rods [4], reinforced fiber plastic [5], scrap tires [6], and PP-band, a polypropylene cord used for packing [7]. All of these are expected to be possible due to the tensile resistance of the materials. PP-band has already been introduced in developing regions because the materials are readily available worldwide, and the construction is easy.

All of the above methods require reinforcement. In contrast, one method that does not require reinforcement is the use of interlocking blocks/bricks [8][9][10]. This reinforcement method is expected to have higher seismic performance than conventional masonry walls, simply by using interlocking blocks/bricks without using reinforcement materials. However, experimental and numerical verification of reinforcement methods using interlocking blocks/bricks are still limited.

Based on the above, this study compares the result of the static loading test and dynamic analysis of masonry walls consisting of rectangular bricks and interlocking bricks and discusses the performance of interlocking bricks. In the dynamic analysis, this study used the refined DEM (distinct element method) [11] rather than the conventional FEM (finite element method) [12].

The FEM is the most common numerical analysis method. It has been used for the analysis of masonry structures [10][12][13][14]. The FEM can deal with both elastic and plastic behaviors, but it has difficulty solving failure and collapse phenomena since it is based on the mechanics of the continuum. A method based on the mechanics of the dis-continuum is more suitable for analyzing failure and collapse phenomena. An example of a numerical method for a dis-continuum is the DEM [15]. However, the DEM also has disadvantages in that the spring constant cannot be determined from the material properties, and the values need to be quantified experimentally [16][17]. Therefore, the reliability of the results is not high. As an alternative, the present paper uses a refined DEM [11][18], where the spring constant of each spring is theoretically determinable. Using the refined DEM, this paper simulates the dynamic behavior of masonry walls consisting of rectangular and interlocking bricks.

2 STATIC LOADING TEST

2.1 Overview

A static loading test of two rectangular brick walls and two interlocking brick walls was conducted to investigate the performance of the interlocking bricks against rectangular bricks.

2.2 Rectangular and interlocking masonry walls

Masonry structures are generally constructed by stacking rectangular bricks, as shown in Fig. 1(a). Failure generally occurs and propagates at joints in rectangular brick walls. When a joint fails, the joint loses resistance other than frictional force and becomes very vulnerable, as shown in Fig. 1(a).

In order to improve the bearing capacity of masonry structures, the use of interlocking bricks has been studied. Assuming that the bricks do not fracture, even if the fracture occurs at joints, the interlocking generates resistant force in addition to friction force, as shown in Fig. 1(b). This resistant force may improve the overall bearing capacity of the masonry structure.

2.3 Masonry wall test specimen

This study considered four types of masonry walls, shown in Fig. 2. Three samples are made for each type. The width, height, and depth of each masonry wall are shown in Table 1. The four types of masonry walls were set to be as close to a square as possible, and the length of one side was as equal as possible. Most of the mortar thickness was 10 mm. However, to keep the masonry walls close to squares, the horizontal joint width was set to 7 mm for the rectangular type 1 and 8 mm for the interlocking types 1 and 2.

Figure 3 shows the dimension of bricks stacked in each type of masonry wall. As shown in Fig. 2, the bricks at the left and right ends of the odd-numbered rows were cut in half. The fabrication errors of several millimeters were observed in the bricks and mortar thickness.

Table 2 shows the material properties and strength obtained by element tests. All elemental tests were conducted three times, and the values were averaged.

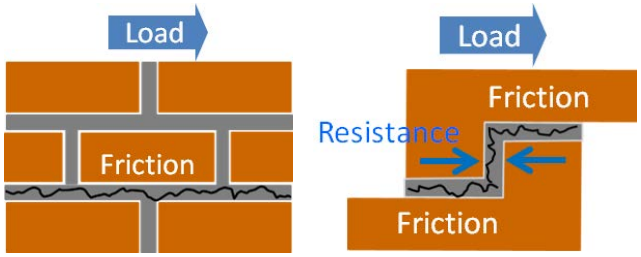

(a)Rectangular brick wall (b)Interlocking brick wall

Figure 1: Rectangular and interlocking brick walls

Table 1: Dimension of masonry walls (unit: mm)

Name	Width	Height	Depth
Rectangular type 1	590	596	100
Rectangular type 2	590	590	100
Interlocking type 1	590	588	100
Interlocking type 2	590	588	100

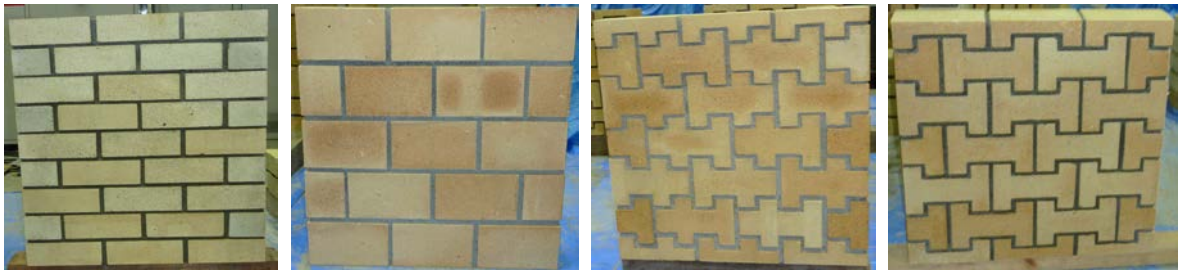

(a) Rectangular type 1 (b) Rectangular type 2 (c) Interlocking type 1 (d) Interlocking type 2

Figure 2: Photographs of masonry walls

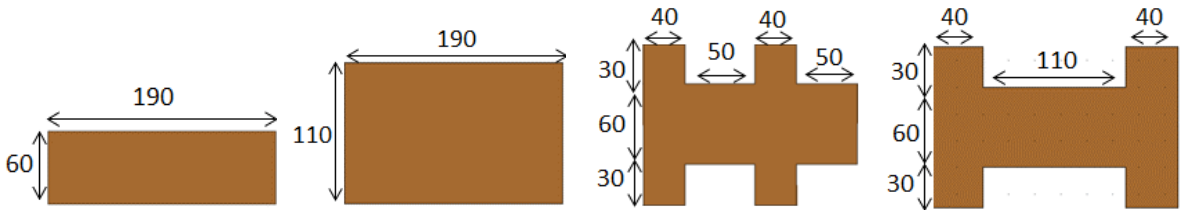

(a) Rectangular type 1 (b) Rectangular type 2 (c) Interlocking type 1 (d) Interlocking type 2

Figure 3: Dimensions of bricks (unit: mm, depth: 10mm)

Table 2: Material properties and strength obtained by element test

(a) Brick and mortar

	Young's modulus (N/m^2)	Poisson's ratio	Compressive strength (N/m^2)	Tensile strength (N/m^2)
Brick (rectangular type 1)	2.04×10^{10}	0.33	2.41×10^{7}	8.84×10^{6}
Brick (except rectangular type 1)	1.69×10^{10}	—	1.69×10^{7}	8.92×10^{6}
Mortar	8.00×10^{8}	0.18	1.69×10^{7}	1.28×10^{6}

(b) Interface between bricks and mortar

Tensile strength (N/m^2)	Bond strength (N/m^2)	Friction coefficient
9.69×10^{5}	1.68×10^{5}	1.25

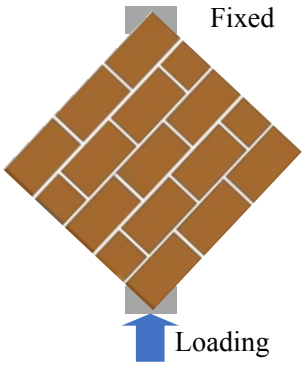

Figure 4: Loading condition

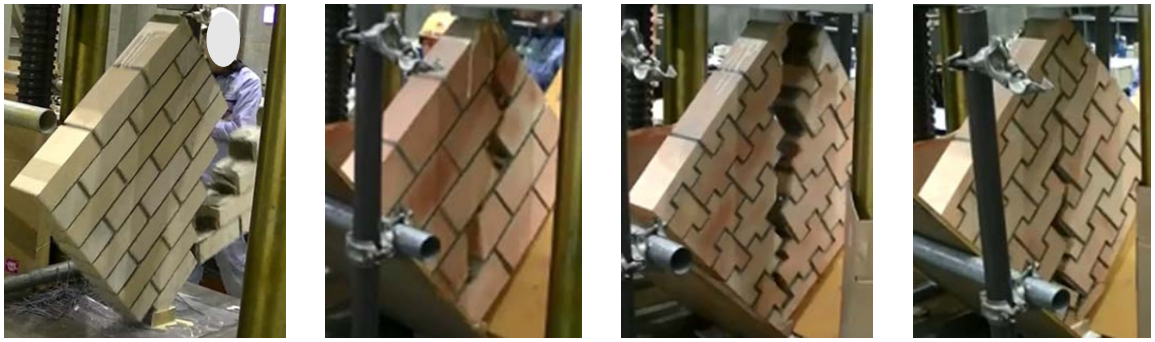

(a) Rectangular type 1 (b) Rectangular type 2 (c) Interlocking type 1 (d) Interlocking type 2

Figure 5: Photographs of masonry walls during loading

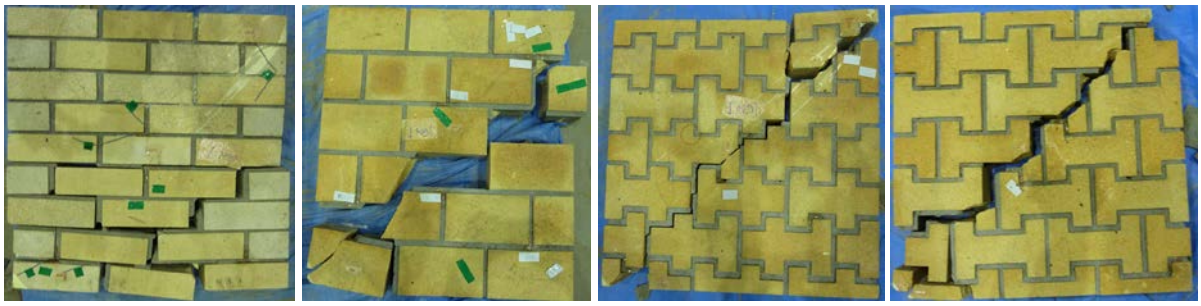

(a) Rectangular type 1 (b) Rectangular type 2 (c) Interlocking type 1 (d) Interlocking type 2

Figure 6: Photographs of masonry walls after loading

2.4 Loading method

Static loading tests were conducted on the four types of masonry wall test specimens. Three specimens of each of the four types were tested. As shown in Fig. 4, M-shaped jigs were attached to the upper and lower loading plates of the universal material testing machine, and the specimen was placed between the jigs.

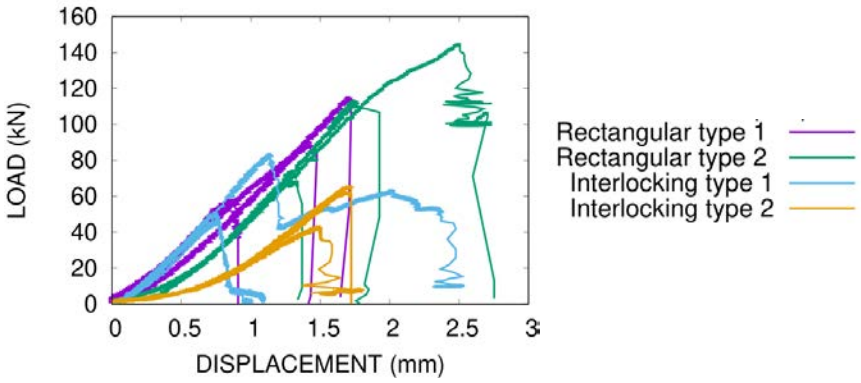

Figure 7: Load-displacement relationship

2.5 Result (Failure pattern)

Three tests were conducted on each of the four different masonry wall models. Photographs of the test specimen during loading are shown in Fig. 5. Photographs of the test specimen after loading are shown in Fig. 6.

In the case of rectangular type 1, the fracture developed on the brick/mortar interface in a stair-step manner. The failure did not occur inside the brick. However, the entire wall collapsed due to the propagation of a fracture on the brick/mortar interface.

In the case of rectangular type 2, the failure propagated in a stair-step manner. Three bricks, one on the bottom and two on the top, got fractured inside the bricks, and the others got fractured in a stair-step manner at the brick/mortar interface (red line). The failure surfaces occurred in the loading direction that connects the upper and lower loading points.

In interlocking types 1 and 2, the failure surface occurred in the loading direction, connecting the upper and lower loading points. The failure occurred at the brick/mortar interface and inside the brick.

2.6 Result (Load-displacement relationship)

The load-displacement relationship is shown in Fig. 7. Three specimens were tested for each type of masonry wall model, shown in the same color.

The three test specimens for the same type have almost the same slope of the load-displacement relationships but different maximum loads. The variation in the maximum load was probably caused by variations in the strength of the bricks and mortar, variations in the strength of the brick-mortar interface, and variations in the setting of the test apparatus.

The maximum load of both interlocking types is smaller than that of both rectangular types.

2.7 Discussion

In the case of the rectangular types, the failure surface mainly developed on the brick/mortar interface. In the case of the interlocking types, the failure surface developed in bricks and on the brick/mortar interface.

The maximum load tended to be lower for the interlocking types than for the rectangular types. The reason for the lower maximum loads in the interlocking types is assumed to be the stress concentration in the bricks in the interlocking area, which facilitates failure.

3 DYNAMIC ANALYSIS

3.1 Overview

Next, the dynamic analysis of the two rectangular brick walls and two interlocking brick walls is performed by the refined DEM to investigate the performance of the interlocking brick walls over the rectangular brick walls.

3.2 Refined DEM

This study employs a refined DEM [11] to simulate a series of structural dynamic behaviors from elastic to failure to collapse phenomena. A structure is modeled as an assembly of rigid elements, and interaction between the elements is modeled with multiple springs and dashpots attached to the elements' surfaces. The elements are rigid, but the method allows the simulation of structural deformation by allowing penetration between elements.

Fig. 8 (a) shows a spring for computing the restoring force (restoring spring), which models the elasticity of elements. The restoring spring is set between continuous elements. Structural failure is modeled as the breakage of the restoring spring, at which time the restoring spring is replaced with a contact spring and a contact dashpot (Fig. 8 (b)). Fig. 8 (b) shows the spring and dashpot for computing the contact force (contact spring and dashpot) and modeling the contact, separation, and recontact between elements. The dashpots are introduced to express energy dissipation due to the contact. Structural collapse behavior is obtained using these springs and dashpots. The elements shown in Figs. 8 (a) and (b) are rectangular parallelepipeds, but the method does not limit the geometry of the elements.

The surface of an element is divided into small segments, as shown in Fig. 8 (c). The segment in the figure is rectangular, but the method does not limit the geometry of the segment. The black points indicate the representative point of each segment, and the relative displacement or contact displacement between elements is computed for these points. Such points are referred to as contact points or master points in this study. One restoring spring and one combination of contact spring and dashpot are attached to one segment (Fig. 8 (d)) at each of the representative points in Fig. 8 (c). The spring constant for each segment is derived based on the stress-strain relationship of the material and the segment area.

The behavior of an element consists of translational and rotational behaviors. Each element's translational and rotational behaviors are computed explicitly by solving Newton’s law of motion and Euler’s equation of motion. Forces acting on each element are obtained by summing the restoring force, contact force, and other external forces, such as the gravitational force and the earthquake’s inertial force.

3.3 Analytical model

The analytical model is shown in Fig. 9. A 70 kg weight is placed on the top of each masonry wall. Figure 10 shows how the brick is modeled in each type of masonry wall. Each brick consists of smaller rectangular elements to account for brick failure. The failure of brick occurs between the element boundary. The failure of mortar occurs between bricks. Figure 11 shows the arrangement of bricks in each model.

The material properties of the rectangular brick type 1 and the material properties of mortar shown in Table 2(a) are used in the analysis. In order to investigate the effect of interlocking mechanisms on the dynamic response, the same material properties of bricks and mortar are used for all the masonry wall models.

As for damping, mass-proportional damping was assumed, and the damping constant was set to 0.03 for the first mode.

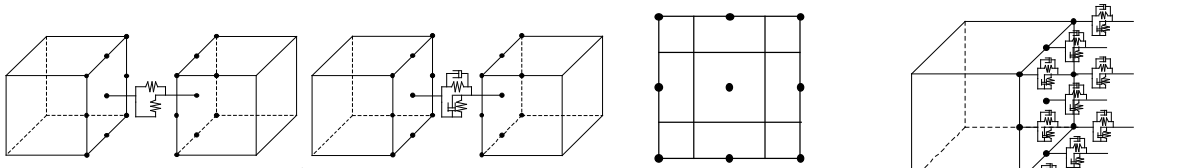

(a) Restoring spring (b) Contact spring/dashpot (c) Segments and contact points (d) Multiple springs/dashpots

Figure 8: Basic concept of the analysis method [11]

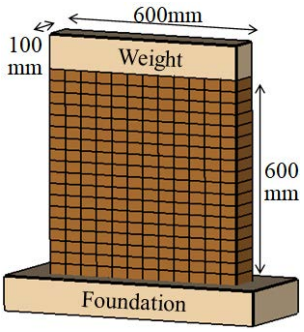

Figure 9: Numerical model

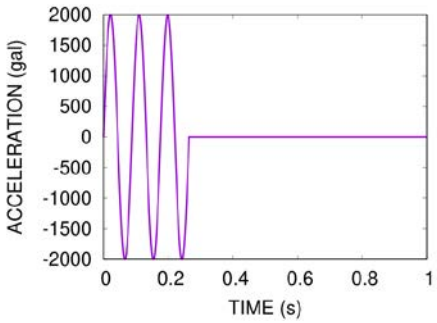

Figure 12: Input acceleration

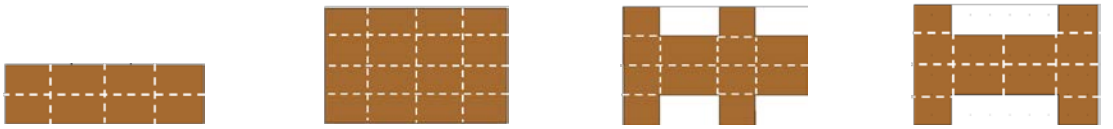

(a) Rectangular type 1 (b) Rectangular type 2 (c) Interlocking type 1 (d) Interlocking type 2

Figure10: Brick model

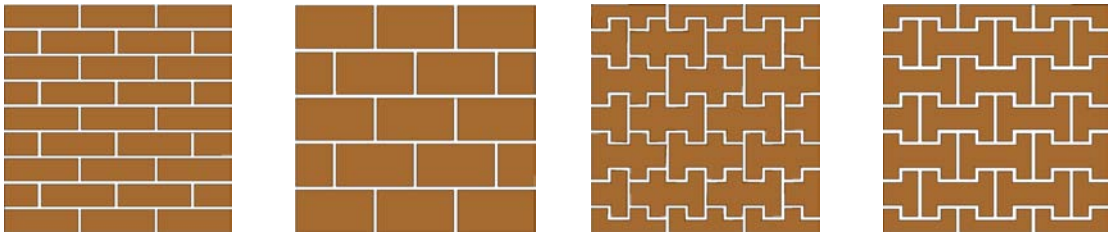

(a) Rectangular type 1 (b) Rectangular type 2 (c) Interlocking type 1 (d) Interlocking type 2

Figure 11: Masonry wall model

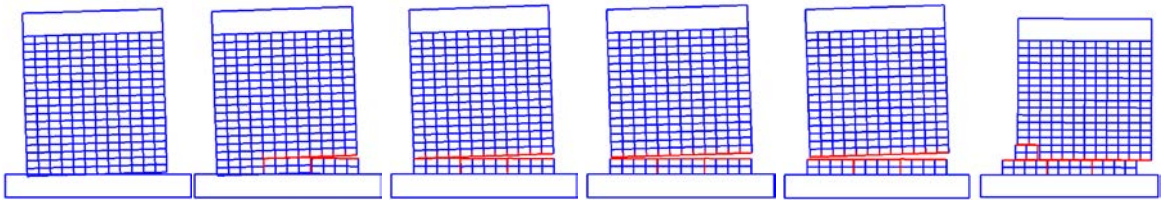

Figure 13: Dynamic behavior of rectangular type 1 (0.22s, 0.23s, 0.24s, 0.25s, 0.26s, 1.0s, from the left)

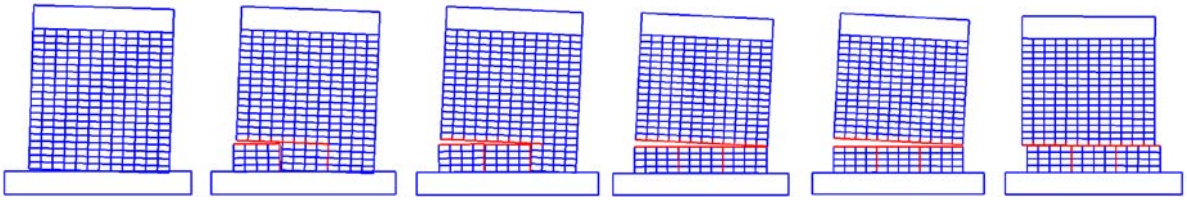

Figure 14: Dynamic behavior of rectangular type 2 (0.26s, 0.27s, 0.28s, 0.29s, 0.30s, 1.0s, from the left)

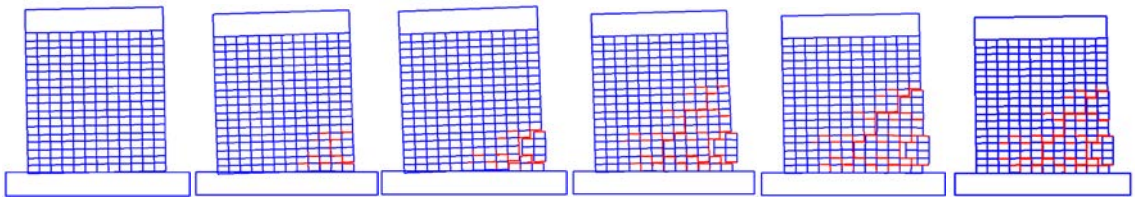

Figure 15: Dynamic behavior of interlocking type 1 (0.21s, 0.22s, 0.23s, 0.24s, 0.25s, 1.0s, from the left)

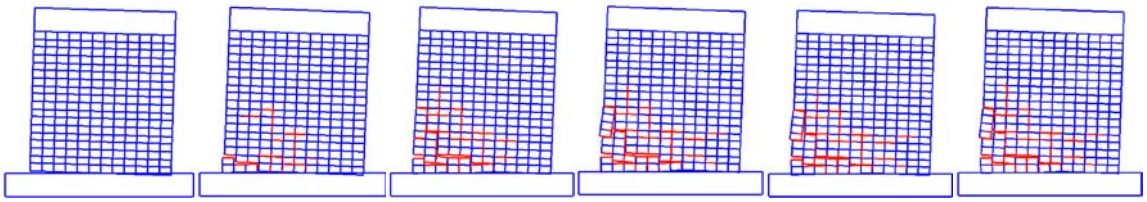

Figure 16: Dynamic behavior of interlocking type 2 (0.26s, 0.27s, 0.28s, 0.29s, 0.30s, 1.0s, from the left)

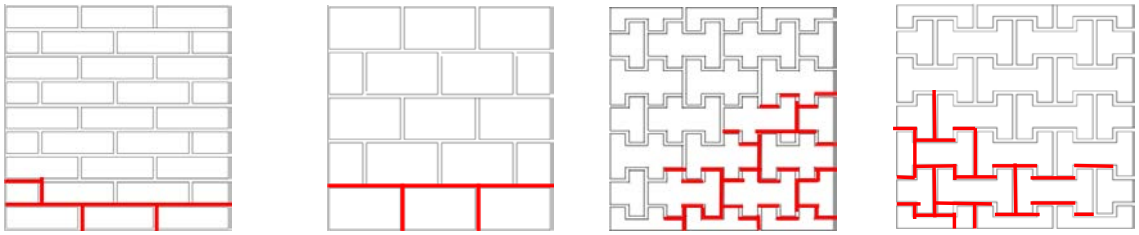

(a) Rectangular type 1 (b) Rectangular type 2 (c) Interlocking type 1 (d) Interlocking type 2

Figure 17: Location of failure after dynamic loading

3.4 Input acceleration

The first mode natural frequency of the analytical model in the in-plane direction was found to be 11.328 Hz through the dynamic analysis of the free vibration. Therefore, three cycles of a sine wave with an amplitude of 2000 gal and a frequency of 11.328 Hz, as shown in Fig.12, were input as ground acceleration in the in-plane direction.

3.5 Result

The process of failure propagation during dynamic loading is shown in Figs. 13-16. The failure location after the dynamic loading is shown in Fig. 17. The red lines indicate where the tensile failure occurred.

In the case of rectangular type 1 (Fig. 13), the failure occurred at 0.23 s at the brick/mortar interface between the lowest and the second lowest bricks on the right side and propagated in the left direction. The failure progressed along the horizontal joints and completely penetrated at 0.24 s. As shown in Fig.17(a), the failure only occurred at the brick/mortar interface, and no failure occurred inside the brick.

In the case of rectangular type 2 (Fig. 14), the failure occurred at 0.27 s at the brick/mortar interface between the lowest and the second lowest bricks on the left side. The failure propagated along the horizontal joints and completely penetrated at 0.29 s. As shown in Fig.17(b), the failure only occurred at the brick/mortar interface, and no failure occurred inside the brick.

In the case of interlocking type 1 (Fig. 15), the failure occurred at 0.22 s at the brick/mortar interface on the right bottom side. The failure then progressed in the wider range compared to rectangular types 1 and 2. As shown in Fig.17(c), the failure occurred at the brick/mortar interface and inside the bricks. Even though the failure occurred in the wider

range and both the brick/mortar interface and the brick itself got failure, the failure propagation stopped during the loading, and the failure surface did not penetrate the brick wall.

In the case of interlocking type 2 (Fig. 16), the failure occurred at 0.27 s on the brick/mortar interface and inside the brick on the left bottom side. Then failure propagated a wider range. Even though the failure occurred in the wider range and both the brick/mortar interface and the brick itself got failure, the failure propagation stopped during the loading, and the failure surface did not penetrate the brick wall, as shown in Fig. 17(d).

Interlocking bricks effectively prevented the cracks from penetrating the masonry wall, although cracking occurs over a wide area of the masonry wall. The interlocking bricks allowed the wall to retain its full shape after the end of the excitation.

4 CONCLUSIONS

This study considered using interlocking bricks as a reinforcement measure for masonry structures as it does not require extra material and is easy to implement. The effectiveness of interlocking bricks instead of regular rectangular bricks is examined by comparing the performance against static loading test and dynamic analysis results using the refined DEM. The static loading test compared the failure behavior and the load-displacement relationship of the masonry walls. The dynamic analysis compared the collapse behavior of the masonry walls against sinusoidal input in the in-plane directions.

The static loading test found that the failure occurred on the brick/mortar interface in the rectangular brick walls, while the failure occurred both on the brick/mortar interface and inside bricks in the interlocking brick walls. It was also found that the interlocking brick walls have a lower maximum load than the rectangular brick walls. The reason is the stress concentration at the interlocking part. The effectiveness of interlocking bricks over rectangular bricks could not be seen in the static loading test.

The dynamic loading analysis observed that the failure only occurred on the brick/mortar interface in the rectangular brick walls. In contrast, the failure occurred in the brick/mortar interface and inside bricks in the interlocking walls. The rectangular brick wall underwent a horizontal crack that penetrated the entire wall and was divided into two pieces. However, the interlocking brick wall suffered cracks in the wider range, but no crack penetration occurred, and the wall was never divided into two parts. The effectiveness of interlocking bricks over rectangular bricks could be seen in the dynamic analysis.

REFERENCES

[1] OCHA: www.unocha.org. [Accessed February 27, 2023].

[2] R.R. Parajuli, A. Furukawa, D. Gautam, Experimental characterization of monumental brick masonry in Nepal. *Structures*, **28**, 1314-1321, 2020. https://doi.org/10.1016/j.istruc.2020.09.065

[3] H.R. Parajuli, J. Kiyono, M. Tatsumi, Y. Suzuki, H. Umemura, H. Taniguchi, K. Toki, A. Furukawa, P.N. Maskey, Dynamic characteristic investigation of a historical masonry building and surrounding ground in Kathmandu. *Journal of Disaster Research*, **6(1)**, Dr6-1-4522, 2011. doi: 10.20965/jdr.2011.p0026

[4] A. Darbhanzi, S. Marefat, M. Khanmohammadi, Investigation of in-plane seismic retrofit of unreinforced masonry walls by means of vertical steel ties, *Construction and Building Materials*, **52**, 122-129, 2014.

[5] G. Marcari, G. Manfredi, A. Prota, M. Pecce, In-plane shear performance of masonry panels strengthened with FRP. *Composites: Part B*, **38**, 887-901 , 2007.

[6] A. Turer, M. Golalm, Scrap tire as low-cost post-tensioning material for masonry strengthening. *Materials and Structures*, **41**, 1345-1361, 2011.

[7] N. Sathiparan, K. Sakurai, K. Meguro, Experimental study of PP-band retrofitted masonry structure made of shapeless stone. *SEISAN-KENKYU*, **61(6)**, 1051-1054, 2009.

[8] A. Furukawa, K. Masuda, J. Kiyono, Diagonal compression test of mortar interlocking masonry wall with various block shapes and different support conditions. *Frontiers in built environment*, **6:579366**, 2020. https://doi.org/10.3389/fbuil.2020.579366

[9] A. Furukawa, J.J. Prasetyo, J. Kiyono, Failure process and load-displacement relationship of rectangular block and interlocking block walls during in-plane lateral loading. *Journal of Japan Society for Natural Disaster Science*, **38**, 25-41, 2019. https://doi.org/10.24762/jndsj.38.S06_25

[10] A. Furukawa, J.J. Prasetyo, J. Kiyono, Performance of interlocking brick walls against out-of-plane excitation. *International Journal of GEOMATE*, **22(89)**, 100-105, 2022. https://doi.org/10.21660/2022.89.gxi413

[11] A. Furukawa, J. Kiyono, K. Toki K, Proposal of a numerical simulation method for elastic, failure and collapse behaviors of structures and its application to masonry walls. *Journal of Disaster Research*, **6(1)**, Dr6-1-4524, 2011. doi: 10.20965/jdr.2011.p0051

[12] P.B. Lourenco, Analysis of masonry structures with interface elements, theory and applications. The Delft University of Technology, Faculty of Civil Engineering, TU-DELFT report no.03-21-22-0-01, 1994.

[13] H.R. Parajuli, J. Kiyono, H. Taniguchi, K. Toki, A. Furukawa, P.N. Maskey, Parametric study and dynamic analysis of a historical masonry building of Kathmandu. *Journal of Disaster Mitigation of Cultural Heritage and Historic Cities*, **4**, 149-156, 2010.

[14] A. Furukawa, J. Kiyono, R.R. Parajuli, H.R. Parajuli, K. Toki, Evaluation of damage to a historic masonry building in Nepal through comparison of dynamic characteristics before and after the 2015 Gorkha Earthquake. *Frontiers in Built Environment*, **3:62**, 2017. doi:10.3389/fbuil.2017.00062.

[15] P.A. Cundall, O.D.L Strack, A discrete numerical model for granular assemblies. *Geotechnique*, **29**, 47-65, 1979.

[16] A. Furukawa, Y. Ohta, Failure process of masonry buildings during earthquake and associated casualty risk evaluation. *Natural Hazards*, 49(1), 25-51, 2009. http://dx.doi.org/10.1007/s11069-008-9275-x

[17] A. Furukawa, R. Spence, Y. Ohta, E. So, Analytical study on vulnerability functions for casualty estimation in the collapse of adobe buildings induced by earthquake, *Bulletin of Earthquake Engineering*, **8(2)**, 451-479, 2010. http://dx.doi.org/10.1007/s10518-009-9156-z

[18] A. Furukawa, J. Kiyono, K. Toki, Numerical simulation of the failure propagation of masonry buildings during an earthquake, *Journal of Natural Disaster Science*, **33(1)**, 11-36, 2012, http://dx.doi.org/10.2328/jnds.33.11